Calcite growth in *Cissus quadrangularis* plant extract, a traditional Indian bone-healing aid

Ambarish Sanyal[1], Absar Ahmad[2] and Murali Sastry[1,3,*]

Nanoscience Group, [1]Materials Chemistry and [2]Biochemical Sciences Division, National Chemical Laboratory, Pune 411 008, India
[3]Present address: Tata Chemicals Limited, Leela Business Park, Andheri-Kurla Road, Andheri, Mumbai 400 059, India

***Cissus quadrangularis*, a plant that has been customarily used in the Indian subcontinent to hasten the process of healing in bone fractures, has been studied and exploited to synthesize calcite crystals. The plant extract serves as a rich source of calcium ions, which when reacted with CO_2, leads to the formation of calcite crystals of highly irregular morphology indicating that bioorganic molecules present in the extract modulate the crystal morphology.**

Keywords: Bone fracture, calcite crystals, *Cissus quadrangularis*, traditional healing.

NATURE relies upon simple mineral crystals to systematically recreate a host of different complex life forms such as gastropods, coccoliths, etc. Among the many inorganic minerals present in biological systems, calcium hydroxyapatite, the major component in bones and teeth, is one of the most important calcium-based minerals due to its biocompatible[1] and biodegradable properties[2]. Consequently, considerable effort has been devoted to understanding how and why this mineralization takes place and a number of biomimetic strategies have been developed to grow calcium hydroxyapatite in the laboratory[3–6]. Some examples include synthesis of high aspect ratio hydroxyapatite nanofibres using reverse micelles under hydrothermal conditions[3]. Apart from traditional methods such as sol-gel synthesis[4] and solid-state reactions[5] more recently, flame synthesis[6] has been employed for synthesizing calcium hydroxyapatite.

Traditional recipes for treatment of physical and mental ailments exist in all major ancient civilizations of the world. One such recipe popular in the Indian subcontinent involves the use of the extract of the plant *Cissus quadrangularis*. The stem and root extracts of this medicinal plant are known to possess antioxidant and antimicrobial activity[7], and are routinely used to accelerate the process of bone-fracture healing[8,9]. In spite of the fact that various organic macromolecules ranging from terpenoids to large stilbene derivatives[10] have been isolated from this plant, few reports exist on its ability to accelerate bone-fracture healing[11]. In this communication, we have analysed the extract of the stem of *C. quadrangularis* from the point of view of its putative ability to promote mineral growth. The stem extract contains a high percentage of calcium ions (ca. 4% by weight) and phosphorus[12], both essential for bone-fracture healing. Furthermore, we show that calcite crystals of interesting morphology may be obtained by simple reaction of the calcium ions present in the extract with CO_2 bubbled directly through the extract.

The broth used in the experiments was prepared by taking 40 g of thoroughly washed and finely cut *C. quadrangularis* stems in a 500 ml Erlenmeyer flask. To the biomass, 100 ml of distilled water was added and then boiled for 5 min. After boiling, the solution was decanted and filtered, and CO_2 was bubbled through 5 ml of the broth. After 3 h of reaction, the originally wheat-coloured solution was observed to turn turbid and after 1 day of reaction, the $CaCO_3$ particles settled down at the bottom of the test tube. The precipitate was filtered, washed with copious amounts of water and redispersed in water. Films of the purified $CaCO_3$ crystals were prepared by simple solution-casting onto Si (111) wafers for scanning electron microscopy (SEM) and energy dispersive analysis of X-rays (EDAX) studies. SEM and EDAX were performed on a Leica Stereoscan-440 instrument equipped with a Phoenix EDAX attachment. X-ray diffraction (XRD) measurements of drop-coated films of the biogenic $CaCO_3$ crystals were carried out on a Phillips PW 1830 instrument operated at a voltage of 40 kV and a current of 30 mA with CuK_a radiation. Fourier transform infrared (FTIR) spectroscopy measurements of the purified and dried biogenic $CaCO_3$ powders taken in KBr pellets were carried out on a Perkin–Elmer Spectrum One instrument at a resolution of 4 cm^{-1}. X-ray photoemission spectroscopy (XPS) measurements of $CaCO_3$ crystals cast in the form of a film on Si (111) substrates were carried out on a VG MicroTech ESCA 3000 instrument at a pressure of better than 1×10^{-9} torr. The general scan and C1s, Ca 2p and P 2p core level spectra were recorded with un-monochromatized Mg K_a radiation (photon energy = 1253.6 eV) at pass energy of 50 eV and electron take-off angle (angle between electron emission direction and surface plane) of 60°. The overall resolution was ~1 eV for XPS measurements. The core level spectra were background-corrected using the Shirley algorithm[13] and chemically distinct species resolved using a nonlinear least squares fitting procedure. The core-level binding energies (BE) were aligned with the adventitious carbon binding energy of 285 eV.

Figure 1 *a* shows a picture of the *C. quadrangularis* plant. The plant possesses a cactus-like overall appearance and grows under arid conditions. Figure 1 *b–d* shows representative SEM images of $CaCO_3$ crystals at different magnifications. At various places on the substrate surface, we could observe quasi-spherical particles of irregular morphology assembled in a linear fashion (Figure 1 *b*, *c*). The size of the particles varies between 3 and 10 μm. While the reasons for the assembly are not understood at this stage, it is possible that it is driven by interactions between biomolecules present on the particle surface. Some of the particles exhibit cube-like and highly elongated ellipsoi-

*For correspondence. (e-mail: msastry@tatachemicals.com)

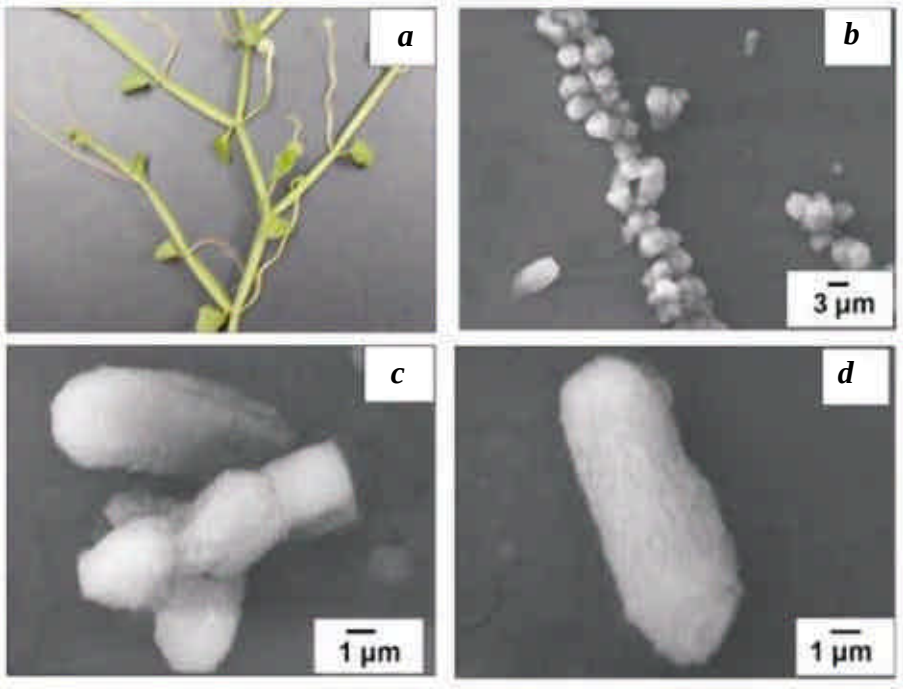

Figure 1. ***a***, Photograph of *Cissus quadrangularis* plant. ***b***–***d***, Representative SEM micrographs at different magnifications of $CaCO_3$ crystals grown from the extract of *C. quadrangularis* plant.

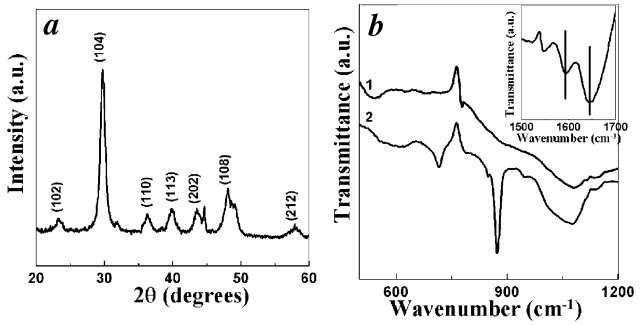

Figure 2. ***a***, XRD pattern recorded from biogenic $CaCO_3$ powder obtained after bubbling CO_2 into the extract of *C. quadrangularis* and subsequent drying. ***b***, FTIR spectra recorded from pure stem extract (curve 1) and from biogenic $CaCO_3$ crystals obtained by bubbling CO_2 into the extract of *C. quadrangularis* (curve 2). (Inset) Region of amide vibrational modes where the amide I and II bands centred around 1590 and 1650 cm^{-1} are identified.

dal morphologies (Figure 1 *d*). All the particles possess a highly irregular and corrugated surface, unlike the smooth, rhombohedral crystals observed in chemically synthesized calcite[14]. Figure 2 *a* shows the XRD pattern recorded from $CaCO_3$ crystals coated on Si (111) substrate. A number of Bragg reflections have been identified and indexed with reference to the unit cell of the pure calcite phase [(*a*, *b*) = 4.989 Å, *c* = 17.062 Å, space group $D_{3D}6$-*R*3*c*][15]. That the morphology of the calcite crystals obtained from *C. quadrangularis* plant extract is significantly different from the one normally observed for calcite indicates the important role of bioorganic molecules present in the extract in modulating the morphology of the crystals. This can be compared to the synthesis of calcite crystals using bovine serum albumin[16] or the self-assembled growth of calcite crystals[17], wherein proteins make an important contribution to the morphological growth of the crystals. It is well known that calcite in biological systems can exist in highly complex morphologies wherein growth in confined reaction spaces and in the presence of specific biomolecules directs the morphology[18,19].

The formation of calcite is further supported by FTIR spectroscopy analysis of the $CaCO_3$ crystals taken in a KBr pellet (curve 2, Figure 2 *b*). For comparison, FTIR spectrum recorded from the lyophilized powder of the plant extract is shown (curve 1, Figure 2 *b*). A comparison of the two curves shows that two strong absorption bands appear at ca. 712 and 870 cm^{-1} in the $CaCO_3$ crystals (curve 2) that are clearly missing in the plant extract (curve 1). These two peaks are characteristic of the pure form of calcite[20]. In order to obtain knowledge about the composition of the crystals, spot-profile EDX was taken (data not shown) and in addition to the C and O signals, an intense Ca signal and peaks corresponding to Mg and P were observed. The presence of Mg may be due to formation of $MgCO_3$. XRD pattern from the crystals shows that the Bragg reflections are broad, most likely due to the presence of $MgCO_3$ that possesses a crystal structure identical to calcite with marginally different lattice spacings[21].

In order to get an idea about the stability of the crystals formed, we have characterized the crystals at different time intervals of growth by SEM (Figure 3). It is observed

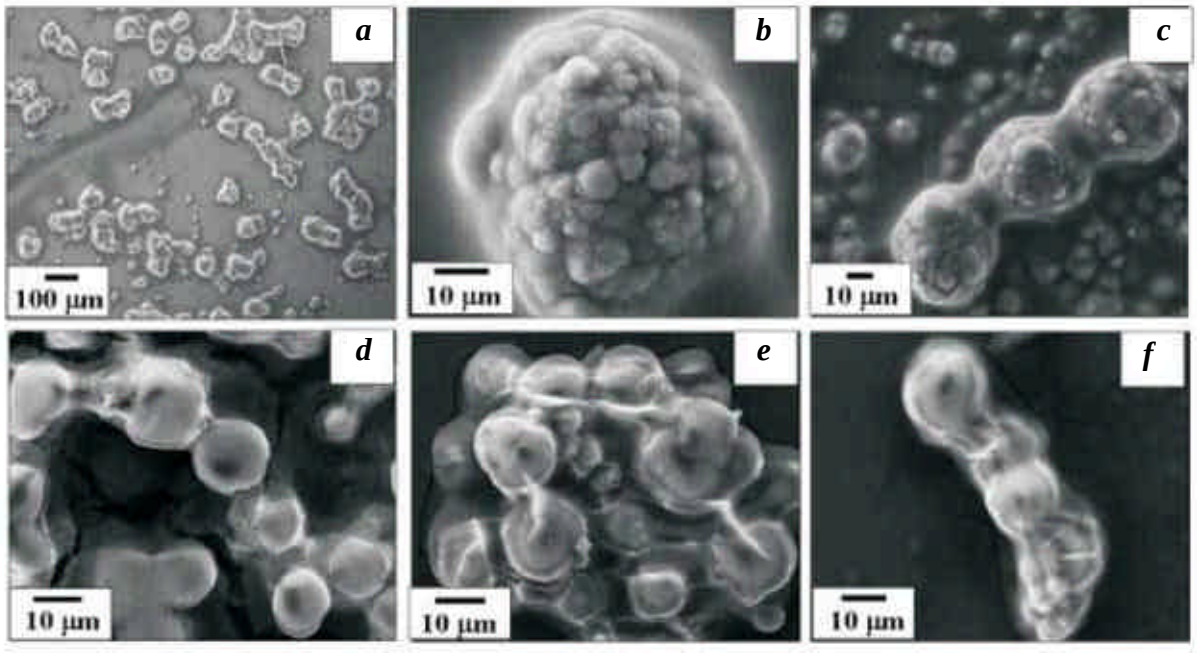

Figure 3. Representative SEM images of calcite crystals formed at different time intervals by bubbling CO_2 into the plant extract of *C. quadrangularis*. ***a***, ***b***, 30 min of reaction; ***c***, ***d***, 2 and 4 h of reaction respectively; ***e***, ***f***, 1 and 2 days of reaction respectively (see text for details).

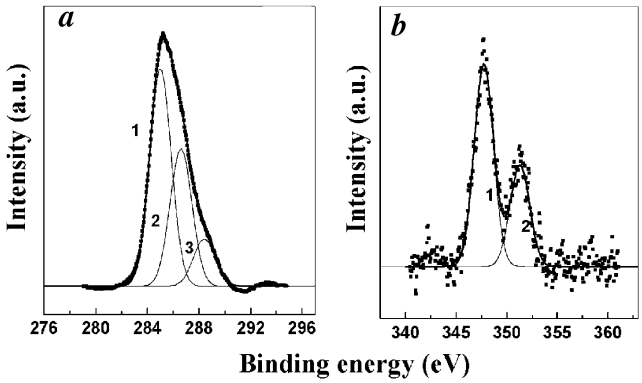

Figure 4. ***a***, C 1s core-level spectrum recorded from a drop-cast film of $CaCO_3$ crystals formed by bubbling CO_2 into the plant extract on a Si (111) substrate together with the chemically distinct components (1–3). ***b***, Ca 2p core-level spectrum recorded from a drop-cast film of calcite crystals synthesized by bubbling CO_2 into the stem extract of *C. quadrangularis* on Si (111) substrate. Curves 1 and 2 correspond to deconvoluted spin-orbit pairs of the 2p component (see text for details).

that after 30 min of reaction, a large number of highly irregular crystals are formed (Figure 3 *a*). At higher magnification, the structures are seen to be composed of sphero-aggregates of much smaller crystals (Figure 3 *b*). As the time of reaction increases, it is observed that the crystals within the superstructures increase in size (Figure 3 *c*, *d*, SEM images recorded after 2 and 4 h of reaction respectively). An interesting observation is that the sphero-aggregates tend to assemble in a linear fashion, similar to the crystals shown in Figure 1 *c*. That the crystals are assembled in a quasi-linear fashion suggests that the biomolecules present are either surface-bound or have been intercalated within the crystal. After 2 days of reaction, the crystallites within the spherical superstructure have recrystallized to yield single particles assembled in a linear manner (Figure 3 *e*, *f*).

Chemical analysis of the calcite crystals grown using *C. quadrangularis* extract and deposited in the form of a film on Si (111) wafers was carried out by XPS. Figure 4 *a* and *b* shows the C 1s and Ca 2p core level spectra respectively. In the C 1s spectrum (Figure 4 *a*), curves 1–3 correspond to the chemically distinct C 1s core levels with BE of 285, 286.6 and 288.4 eV respectively. These BE most likely originate from the hydrocarbon chains, ***a***-carbon and keto (–C=O) groups present in the protein fraction of the aqueous extract. That the proteins are present on the surface of the calcite crystals is also supported by the presence of amide vibrational modes (amide I and II bands centred at around 1590 and 1650 cm^{-1}) in the FTIR spectrum of the crystals (inset, Figure 2 *b*). We believe these proteins are responsible for modulation of morphology of the calcite crystals (Figure 1 *b–d*). The Ca 2p core-level spectrum (Figure 4 *b*) could be resolved into one spin-orbit pair (splitting ~ 3.55) with a $2p_{3/2}$ BE of 347.7eV. This BE is characteristic of calcium carbonate[22]. A weak P 2p signal was also recorded from the calcite crystals (data not shown). However, the signal-to-noise ratio of this core level was not sufficient to perform a reliable quantitative analysis.

In conclusion, we have shown here the formation of truly biogenic $CaCO_3$ crystal of exquisite morphology by simply bubbling CO_2 into the aqueous stem extract of an indigenous medicinal plant, *C. quadrangularis*. The plant contains a

high percentage of calcium probably due to its thick cell wall, which makes it suitable for growth of mineral crystals. The presence of phosphorous in the plant can also be exploited for synthesizing hydroxyapatite, thus utilizing the traditional knowledge of bone-fracture healing in advanced technique of new material synthesis.

1. Habibovic, P., Barrere, F., Van Blitterswijk, C. A., De Groot, K. and Layrolle, P., Biomimeitic hydroxyapatite coating on metal implants. *J. Am. Ceram. Soc.*, 2002, **85**, 517–522.
2. Lu, J. X., Descamps, M., Dejou, J., Koubi, G., Hardouin, P., Lemaitre, J. and Proust, J.-P., The biodegradation mechanism of calcium phosphate biomaterials in bone. *J. Biomed. Mater. Res.*, 2002, **4**, 408–412.
3. Cao, M., Wang, Y., Guo, C., Qi, Y. and Hu, C., Preparation of ultrahigh aspect-ratio hydroxyapatite nanofibers in reverse micelles under hydrothermal conditions. *Langmuir*, 2004, **20**, 4784–4786.
4. Jillavenkatesa, A. and Condrate, R. A. S. R., Sol-gel processing of hydroxyapatite. *J. Mater. Sci.*, 1998, **33**, 4111–4119.
5. Yang, X. H. and Wang, Z. H., Synthesis of biphasic ceramics of hydroxyapatite and *b*-tricalcium phosphate with controlled phase content and porosity. *J. Mater. Chem.*, 1998, **8**, 2233.
6. Loher, S. *et al.*, Fluoro-apatite and calcium phosphate nanoparticles by flame synthesis. *Chem. Mater.*, 2005, **17**, 36–42.
7. Murthy, K. N. C., Vanitha, A., Swami, M. M. and Ravishankar, G. A., Antioxidant and antimicrobial activity of *Cissus quadrangularis* L. *J. Med. Food*, 2003, **6**, 99–105.
8. Udupa, K. N. and Prasad, G. C., Further studies on the effect of *Cissus quadrangularis* in accelerating fracture healing. *Indian J. Med. Res.*, 1964, **52**, 26–35.
9. Chopra, S. S., Patel, M. R. and Awadhiya, R. P., Studies of *Cissus quadrangularis* in experimental fracture repair: a histopathological study. *Indian J. Med. Res.*, 1976, **64**, 1365–1368.
10. Adesanya, Saburi, A., Rene, N., Martin, M-Therese, Boukamcha, N., Montagnac, A. and Pais, M., Stilbene derivatives from *Cissus quadrangularis*. *J. Nat. Prod.*, 1999, **62**, 1694–1695.
11. Deka, D. K., Lahon, L. C., Saikia, J. and Mukit, A.., Effect of *Cissus quadrangularis* in accelerating healing process of experimentally fractured radius–ulna of dog: A preliminary study. *Indian J. Pharmacol.*, 1994, **26**, 44–45.
12. Enechi, O. C. and Odonwodo, I., An assessment of the phytochemical and nutrient composition of the pulverized root of *Cissus quadrangularis*. *Bio-Research*, 2003, **1**, 63–68.
13. Shirley, D. A., High-resolution X-ray photoemission spectroscopy of the valence bands of gold. *Phys. Rev. B*, 1972, **5**, 4709–4714.
14. DeOliviera, D. B. and Laursen, R., Control of calcite morphology by a peptide designed to bind to a specific surface. *J. Am. Chem. Soc.*, 1997, **119**, 10627–10631.
15. The XRD patterns were indexed with reference to the unit cell of the calcite structure; ([*a*, *b*) = 4.989 Å, *c* = 17.062 Å, space group $D_{3D}6$-*R*3*c*, ASTM chart card no. 5-0586].
16. Nayar, S. and Sinha, A., Protein-induced morphosynthesis of calcium carbonate. *J. Mater. Sci. Lett.*, 2003, **22**, 167–170.
17. Sinha, A., Chakraborty, J., Das, S. K. and Ramachandrarao, P., Self-assembled growth of calcite particles on a tobacco film. *Curr. Sci.*, 2003, **84**, 1437–1440.
18. Kato, T., Sugawara, A. and Hosoda, N., Calcium carbonate-organic hybrid materials. *Adv. Mater.*, 2002, **14**, 869–877.
19. Feng, Q. L., Pu, G., Pei, Y., Cui, F. Z., Li, H. D. and Kim, T. N., Polymorph and morphology of calcium carbonate crystals induced by proteins extracted from mollusk shell. *J. Cryst. Growth*, 2000, **216**, 459–461.
20. Rautaray, D., Sainkar, S. R. and Sastry, M., Ca^{2+}-Keggin anion colliodal particles as templates for the growth of star-shaped calcite crystal assemblies. *Langmuir*, 2003, **19**, 10095–10099.
21. Magnesium carbonate is of the space group $D_{3D}6$-*R*3*c*, with crystallographic axis (*a*, *b*) = 4.633 Å, *c* = 15.01 Å, PCPDF file no. 08-0479, CAS no. 13717-00-5.
22. Muilenberg, G. E. *et al.*, In *Handbook of X-ray Photoelectron Spectroscopy*, Perkin-Elmer Corporation, 1979, p. 64.

ACKNOWLEDGEMENTS. A.S. thanks the Council of Scientific and Industrial Research (CSIR), Govt of India for a research fellowship.

Received 23 May 2005; revised accepted 3 October 2005

Molecular characterization of *Humicola grisea* isolates associated with *Agaricus bisporus* compost

S. K. Singh*, B. Vijay, Vishal Mediratta, O. P. Ahlawat and Shwet Kamal

National Research Centre for Mushroom, Chambaghat, Solan 173 213, India

Composite compost samples were collected from Solan, Sonepat, Gangtok, Kaithal, Phagwara and Ooty, at different stages of *Agaricus bisporus* compost preparation by long and short methods using a variety of agro-waste substrates. Eight isolates of *Humicola grisea* were retrieved on yeast agar medium at 45 and 52°C. PCR amplification of internal transcribed spacer (ITS) region of 5.8S ribosomal RNA (rRNA) gene was done using ITS-1 and ITS-4 primers. An ITS fragment of approximately 550 bp was amplified from all the eight *H. grisea* isolates with no intra-specific diversity in the ITS region of 5.8S rRNA gene. RAPD genotyping was performed using five decamer primers. Combined phylogenetic analysis of RAPD profiles of *H. grisea* by five primers depicted intra-specific variation amongst the eight isolates and divided these into five distinct sub-clades. Molecular analysis carried out in the present study would suggest that isolates within this species exhibit genetic differences, which correlates well with morphological variations.

Keywords: *Agaricus bisporus*, compost microflora, genetic diversity, *Humicola grisea*, RAPD.

AGARICUS bisporus (white button mushroom) grows on compost, a product of aerobic fermentation by various microorganisms. These microorganisms convert and degrade straw to lignin humus complex, which is later utilized by the mushroom mycelium and ultimately contributes to the nutrition of *A. bisporus*[1,2]. The thermophilic fungi play a

*For correspondence. (e-mail: sksingh1111@hotmail.com)